SPACE TELESCOPE SCIENCE INSTITUTE
Operated for NASA by AURA

Instrument Science Report WFC 2015-02

Standard Astrometric Catalog and Stability of WFC3/UVIS Geometric Distortion

V. Kozhurina-Platais, & J. Anderson

March 11, 2015

Abstract

Observations of the globular cluster ω Cen taken with the WFC3/UVIS F606W over a 5-year time period have been used to create a standard astrometric catalog in the central region of this cluster. The newly created catalog is then used to examine the linear part of the WFC3/UVIS distortion solution and to search for variations of the astrometric X&Y scale over time. The variations of the X&Y scale over time have been examined with X&Y positions derived from single UVIS drizzled images, based on Kozhurina-Platais (2014) geometric distortion solution in the form of the reference IDCTAB file for ST software DrizzlePac/AstroDrizzle and ST OPUS pipe-line. The main results of this examination are: 1) over the 5-year time period of WFC3 operations, the WFC3/UVIS distortion is found to be time–independent; 2) there is no sudden or extreme fluctuations in the WFC3/UVIS astrometric scale; 3) the geometric distortion solution over this period time is accurate at the level of ± 2 mas.

1. Introduction

Wide Field Camera 3 (WFC3), a fourth-generation imaging instrument, was installed on *HST* during Servicing Mission 4 in May 2009. An optical ray-tracing model predicted significant geometric distortion in the WFC3/UVIS camera, on the order of $\sim 7\%$ across the detector. This distortion amounts to as much as 120 pixels or $\sim 5''$ in the WFC3/UVIS

[1]Copyright © 2003 The Association of Universities for Research in Astronomy, Inc. All Rights Reserved.

channels. The accuracy of the geometric distortion model is important not only for deriving accurate positions, parallaxes and proper motions of scientifically interesting objects but also to rectify the WFC3 images and to combine them into a common frame. The ST *DrizzlePac/AstroDrizzle* software (Gonzaga *et al.* 2012), currently installed in the STScI on-the-fly pipeline (OTFR), requires an accurate distortion correction in order to combine dithered WFC3/UVIS images, to reject cosmic rays, to enhance the spatial resolution, and to deepen the detection limit. Any significant uncertainty in the geometric distortion correction is therefore detrimental to the alignment of WFC3 images with *DrizzlePac/AstroDrizzle* software.

One of the main uncertainties in the geometric distortion is a potential variation of the $X\&Y$ scale over time. The $X\&Y$ scale presented by linear terms in the ACS/WFC geometric distortion have monotonically changed since the ACS was installed in 2002, as shown by Anderson (2007). The size of this change is clearly noticeable over 5 years, reaching about 15 *mas* (0.3 pixel) off from the original 2002-year-based distortion solution. This level of uncertainty in the ACS/WFC distortion model will introduce a poor and inaccurate alignment of drizzled ACS/WFC images with new *DrizzlePac/AstroDrizzle* software. In contrast to ACS/WFC, the early results from one year of the WFC3/UVIS observations (Kozhurina-Platais, *et.al.* 2010), and later from 2 years of observations (Kozhurina-Platais & L. Petro, 2012) showed that the WFC3/UVIS $X\&Y$ scale are stable within of 0.05 UVIS pixel (2 *mas*). Even so, it is important to re-examine and monitor the WFC3 $X\&Y$ scale and forecast the evolution of the scale of the geometric distortion with time using a longer 5-year baseline. Any changes in the linear part of geometric distortion with time would also be an indication of mechanical, optical, and thermal changes in the WFC3 camera itself.

The WFC3/UVIS & IR geometric distortion, as described in Kozhurina-Platais *et al.* (2009), is based on two astrometric reference frames in the vicinity of globular cluster *47Tuc* and *The Large Magellanic Cloud (LMC)* field. In Cycle 18 (2010), an astrometric catalog based on ACS/WFC observations of the globular cluster ω *Cen* was used to examine and derive the multi-wavelength geometric distortion of the WFC3/UVIS and IR channel (Kozhurina-Platais *et al.* 2012). The tangential–plane positions of stars in this catalog are given at the average epoch of 2006 and are accurate to $\sim$0.02 ACS/WFC pixel (0.1 *mas*) across of the entire catalog (Anderson & van der Marel 2010). The internal velocity dispersion in proper motions of ω *Cen* is at the level of 0.9 *mas* per year, as reported by Anderson & van der Marel (2010), hence, the epoch difference of 4 years contributes to the degradation of X&Y positions as much as 4 *mas* and more. For this reason, the astrometric catalog in the vicinity of ω *Cen* based on epoch of 2006 positions has to be updated to the current epoch taking into account the motions of stars.

The aim of this paper is two–fold. First, it attempts to derive a new standard astrometric frame in the central region of globular cluster ω *Cen* based on the current observations with WFC3/UVIS and combined with the early ACS/WFC observations in order to obtain proper

motions of stars in this stellar cluster and then to be used for correcting the positions of stars. Second, it aims to examine the linear part of the WFC3/UVIS distortion by comparing with this newly-derived standard astrometric frame.

Here, we present the construction, analysis and results of the standard astrometric frame and associated proper motions in the central region of ω *Cen* and its application to the study of WFC3/UVIS geometric distortion variation over a 5-year time period.

2. Observations

All available observations of ω *Cen* taken with the WFC3/UVIS through the F606W filter (chosen as an astrometric reference filter) over a 5-year lifetime were used to create an accurate astrometric catalog and allow us to look then for a potential time-dependent evolution in the linear terms of geometric distortion.

Table 1 provides the basic information of these ω *Cen* observations, such as the HST calibration program ID, date of observations, α and δ (in decimal degrees) of the field center, dither pattern defined in the *POS TARG* parameter, the HST roll-angle *PA_V3*, number of observations and the total exposure time. Several special geometric distortion calibration programs listed here were designed so that ω Cen would be observed through the F606W filter with the same pointing but the roll-angle would be changed from a nominal roll–angle *PA_V3* at the $\pm$15°steps. During the second-epoch observations of the calibration program CAL-11911, there were problems with guide-star acquisition that resulted in the loss of several images in F606W filter, which were repeated later.

In all, there are 81 UVIS frames for inter-comparison, all of them with different *POS TARGs* and different orientation. If the relating frames had been obtained with the same pointing and orientation, any errors in the geometric distortion would have canceled out, but such errors would be detectable in frames taken with different pointing and orientations. A variety of *POS TARGs* and different roll-angles are important conditions in order to investigate any systematic errors in the X&Y positions corrected for distortion.

Table 1: UVIS Observations of ωCen

Proposal	Date yy-mm-dd	α (°)	δ (°)	POSTARGS (″)	PA_V3 (°)	Δ(PA_V3) (°)	Number of Images	Exp Sec
11452	2009-07-15	201.6968	-47.47956	0	286.8	0	1	35
11911	2010-01-14	201.6928	-47.47905	±40	105.0	0	9	360
11911	2010-04-29	201.6928	-47.47955	±40	199.9	0	9	360
11911	2010-04-29	201.6928	-47.47955	±40	199.9	0	9	360
11911	2010-04-29	201.6928	-47.47955	±40	279.9	0	9	360
12094	2010-04-25	201.6928	-47.47905	0	219.9	±10	9	360
12339	2011-02-14	201.6928	-47.47905	±40	139.9	0	9	360
12353	2010-12-12	201.6928	-47.47905	0	83.1	0	2	80
12353	2011-03-20	201.6928	-47.47905	0	137.9	+5/+20	6	240
12353	2011-07-25	201.6928	-47.47905	0	275.9	+10/+5	5	200
12694	2012-02-27	201.6928	-47.47905	0	133.8	0	1	350
12694	2012-04-27	201.6928	-47.479055	0	203.3	0	1	350
12714	2012-03-08	201.6929	-47.479055	0	136.9	+10	4	240
13100	2012-12-14	201.6929	-47.479055	±40	84.9	0	3	144
13100	2013-02-02	201.6929	-47.479055	±40	129.9	0	3	144
13100	2013-03-14	201.6929	-47.479055	0	135.9	+15	3	120
13100	2013-03-24	201.6929	-47.479055	0	174.8	0	3	144
13570	2013-12-13	201.6929	-47.479055	0	79.3	+10	3	120
13570	2014-04-05	201.6929	-47.479055	0	169.9	±18	3	120
13570	2014-09-06	201.6929	-47.479055	0	318.3	±5	3	120

3. Standard Astrometric Catalog

The easiest way to see distortion in a particular observed frame is to compare the positions of stars in that frame against positions of stars in a distortion-corrected frame, free of any systematic errors and, a so–called "standard astrometric catalog". After applying only a 4-parameter conformal transformation (two for offset, one for rotation, one for scale), between X&Y positions from standard astrometric catalog and X&Y positions in any particular frame, any residuals in the X&Y positions should be indicative of the frame's uncorrected distortion.

The first step, thus, is to construct an astrometric standard catalog of the stars in the central region of globular cluster ω *Cen*. This is useful for the purpose of the current investigation and for the future calibrations of any detectors. It is not easy to make a good astrometric reference frame for one detector and for use with another, since each detector has a different field of view, a different plate–scale, a different sensitivity, and a different measurement precision. Existing astrometric catalogs can often help in the construction of a reference frame for a detector in order to calibrate it in an absolute sense (to define a set of axes by which to measure the position, orientation and scale) and to set the initial linear terms of the solution. But in the end, it is usually the case that a detector must help in its own distortion calibration. This is called "self-calibration". Here we will pursue a self-calibration strategy for WFC3/UVIS, generating an astrometrically accurate reference frame at the center of globular cluster ω *Cen* and using it later to examine any systematic errors in the official geometric distortion for the WFC3/UVIS.

3.1. Analysis and Setup the Reference Frame

All observations of ω *Cen* listed in Table 1 were used to construct an accurate and precise astrometric standard catalog. In order to do this, first, we have to derive accurate and precise X&Y positions from each individual UVIS exposure. It is a well known fact that the Charge Transfer Efficiency (CTE) of the UVIS detector has inevitably been declining over time as on-orbit radiation damage creates charge traps in the CCDs. The CTE losses introduced not only a loss of flux but also a centroid shift, the amplitude of which depends on the star's signal level and position on the CCD chip (Kozhurina-Platais *et al.* 2007). CTE-induced centroid shifts in X&Y positions are typically on the order of $\sim$0.1, and declining with time. This amount of centroid shifts is significant for high-precision astrometry. To correct for CTE-induced centroid shift, all UVIS observations, listed in Table 1, were processed through the pixel-based CTE correction[1], that has been constructed for the UVIS detector. The WFC3/UVIS images corrected for pixel-based CTE are renamed `*_flc.fits` images instead of the standard output from HST pipe line as (`*_flt.fits`). The pixel-based CTE correction is not yet implemented in the CALWF3 pipe line and is available only through WFC3 web-page[2].

The accuracy of measured X&Y positions also depends critically on the accuracy of the PSF model representing the UVIS PSF, which is under-sampled and spatially variable across the UVIS CCD chips. Anderson & King (2000) developed a purely empirical model (which they called the *effective* PSF or ePSF) to describe the WFPC2 PSF and do high-precision photometry and astrometry in WFPC2 images. In 2006, they extended this model

[1]The correction is based on the Anderson & Bedin (2010) algorithm

[2]http://www.stsci.edu/hst/wfc3/tools/cte_tools

to ACS/WFC (Anderson & King 2006) and represented its spatial variation with an array of 9×5 fiducial PSFs across each ACS/WFC CCD. Similar treatment was used to construct an array of 7×4 PSFs across each UVIS chip[3]. The software img2xym_wfc3uv.F, (available at the WFC3 web-site[4]), uses these UVIS PSFs to find and measure stars in images. The finding parameters were set to identify every pixel that had no brighter pixels within a radius of 4 and at least 1000 e^- counts over sky within its central 2×2 pixels as a potential stars. The central 5×5 pixels were then fit with the local PSF to determine a position and flux. The output from the routine is the list of X&Y positions and flux for each star from the UVIS images. These derived X&Y positions were corrected for the geometric distortion based on the solution provided in Bellini *et al.* (2011), which is better than 0.008 UVIS pixel (0.3 *mas*) in each coordinate.

These precise X&Y positions, corrected now for distortion, will be used for construction of an astrometric reference frame. The initial reference frame was chosen as the catalog of ω *Cen* based on ACS/WFC observations and derived by Anderson & van der Marel (2010) from HST GO-10775 (PI Sarajedini) program. This catalog simply provides an initial coordinate system or set of axes, the zero-point and orientation for the frame, with the plate–scale of 50 *mas*.

The derived UVIS X&Y positions were matched against the catalog to construct a preliminary mapping from each UVIS exposure into the initial reference frame. It is important to note here, that the Bellini geometric distortion solution was based on early observations of ω *Cen* in F606W UVIS filter, and because of that, the geometric solution was not able to pin down the linear terms of the solution perfectly. In the course of this work, it was found that the on-axis skew term (representing the difference in scale between X&Y axis) of the Bellini solution have be to adjusted by 0.02 pixel in order to best match the UVIS positions:

$$\mathrm{X_{new}} = \mathrm{X_{old}} + (\mathrm{X_{old}} - 2048)/2048 \times 0.001 \quad (1)$$

$$\mathrm{Y_{new}} = \mathrm{Y_{old}} - (\mathrm{Y_{old}} - 2048)/2048 \times 0.001 \quad (2)$$

Finally, we found that some of the stars in the UVIS exposures extended into negative coordinates in the reference frame, so adjusting the frame by adding 1000 pixels in each coordinate, the final frame is subtended by 8000×8000 pixel with the true center of the cluster at (3725, 3810).

[3]http://www.stsci.edu/WFC3/WFC3UV.PSFs

[4]http://www.stsci.edu/WFC3/

3.2. Construction of Master Stars List

Now that we have an initial reference frame and accurate distortion-corrected positions in many independent frames, we are ready to pursue our "self–calibration" strategy for the WFC3/UVIS in order to generate an accurate reference frame at the center of ω *Cen*.

In order to construct a single master star list from the 81 independent X&Y positions lists, we mapped each found source from each of the UVIS exposures into the reference frame and identified a catalog star wherever a star could be found in at least half of the available exposures. The process of finding good reliable measured stars is not straightforward since among the good stars there are cosmic rays and other spurious sources in the inhomogeneous coverage over 80 exposures in the central region. Figure 1 shows a map of the depth of coverage from all UVIS images, listed in Table 1. A star at the center of the field can be measured in over 81 exposures and therefore will have a very well constrained positions, but the number of exposures for star far from the center can drop to about 10 exposures. Thus, this procedure resulted in finding 184,890 well-measured stars.

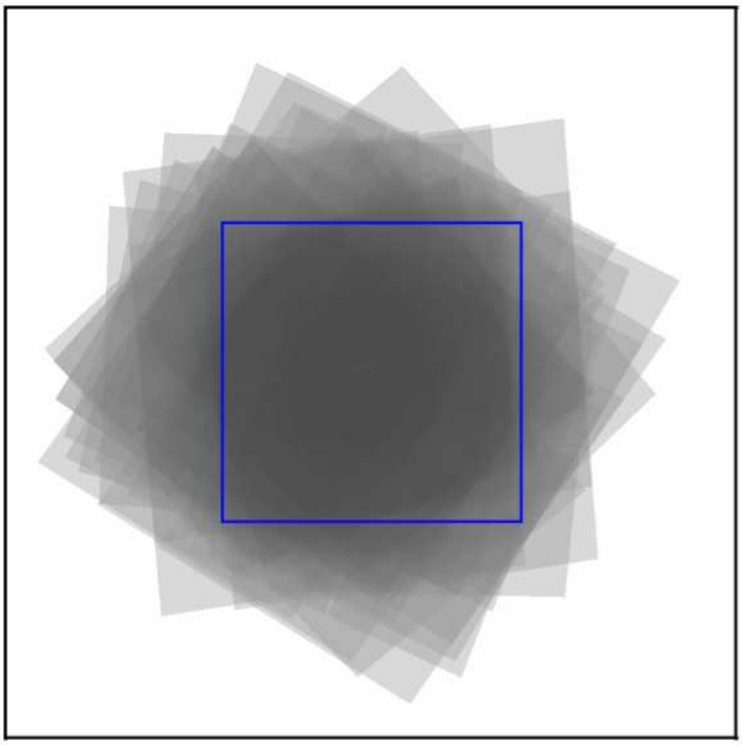

Fig. 1.— Map of the depth of coverage from all F606W UVIS filter observations. The black square is the boundary of the initial reference frame and the blue square is roughly the size of the UVIS field of view. The gray area shows a very heterogeneous data set.

The globular cluster ω *Cen* is the largest globular cluster in Miky Way with very gradually and moderately compressed to the center. The core radius of the cluster $\sim 2\farcm37$ (Harris, 1996) is similar to the size of field-of-view of the WFC3/UVIS images ($2\farcm7 \times 2\farcm7$). Since all ω *Cen* observations were taken in the center of the cluster, there is only a weak density change along the radial direction of density profile in any of our UVIS images and because of that there is no strong evidence of the stellar radial density profile. As seen in Figure 2, the stars have a nice, flat distribution, indicating a homogeneous star list from a very heterogeneous data set.

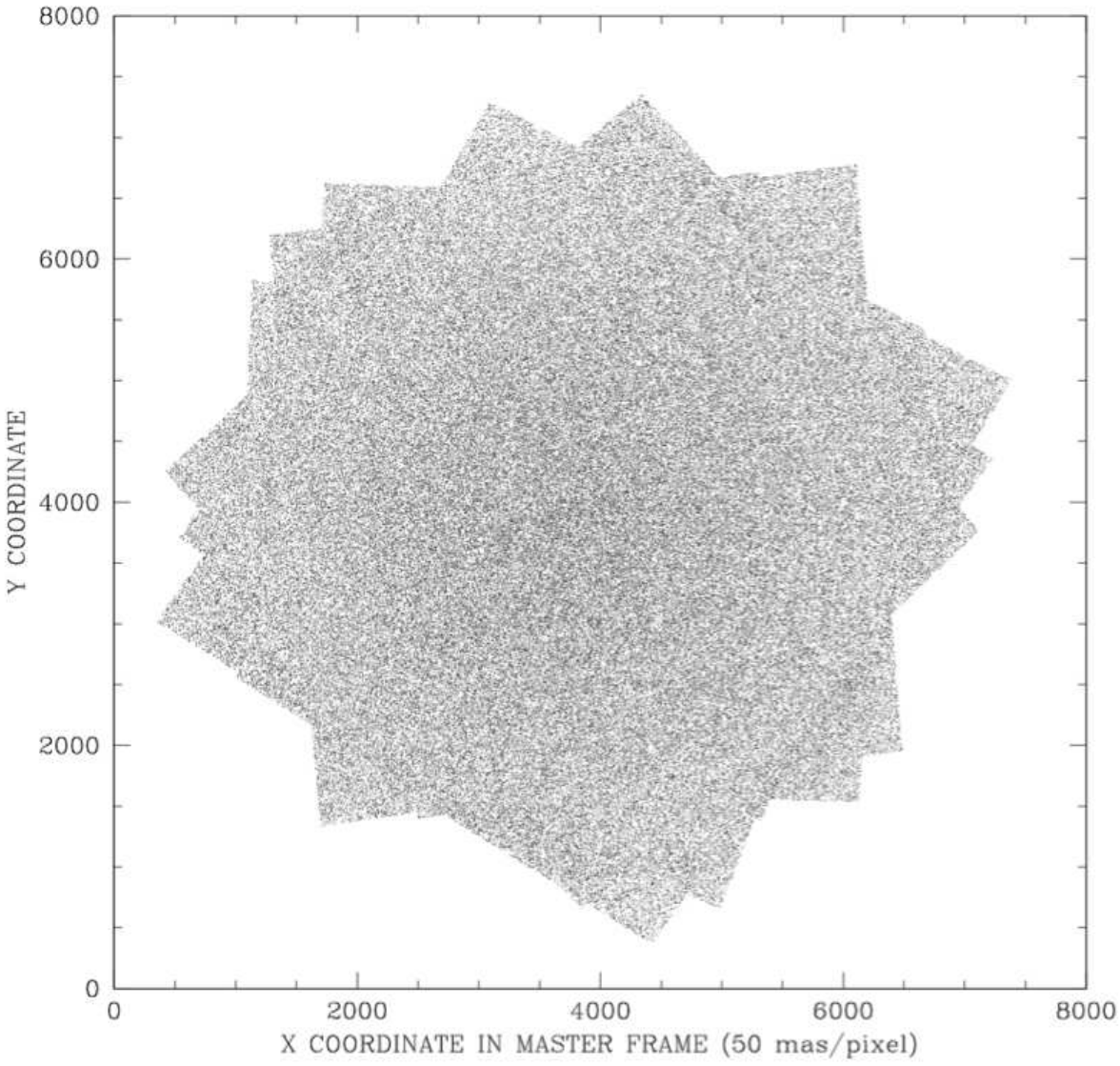

Fig. 2.— X&Y positions of 184,890 well–measured stars in the master stars list. The X and Y coordinates are given in ACS/WFC pixel.

All UVIS images used for creating the master stars list, were stacked into a non-photometric but representative image of the field, with a header that has all the relevant WCS information. This stack image is available to the public for the future work with UVIS images as an astrometric reference image and/or to be used with the ST software *DrizzlePac/AstroDrizzle*. Figure 3 (left panel) shows the stacked image made from all 81 UVIS exposures of ω *Cen* and the right panel shows a close-up the region around the cluster center. It is clear that the created master star list does not identify all stars, but rather focuses on the bright, isolated stars that can be measured well in the 40s F606W exposures we have access to.

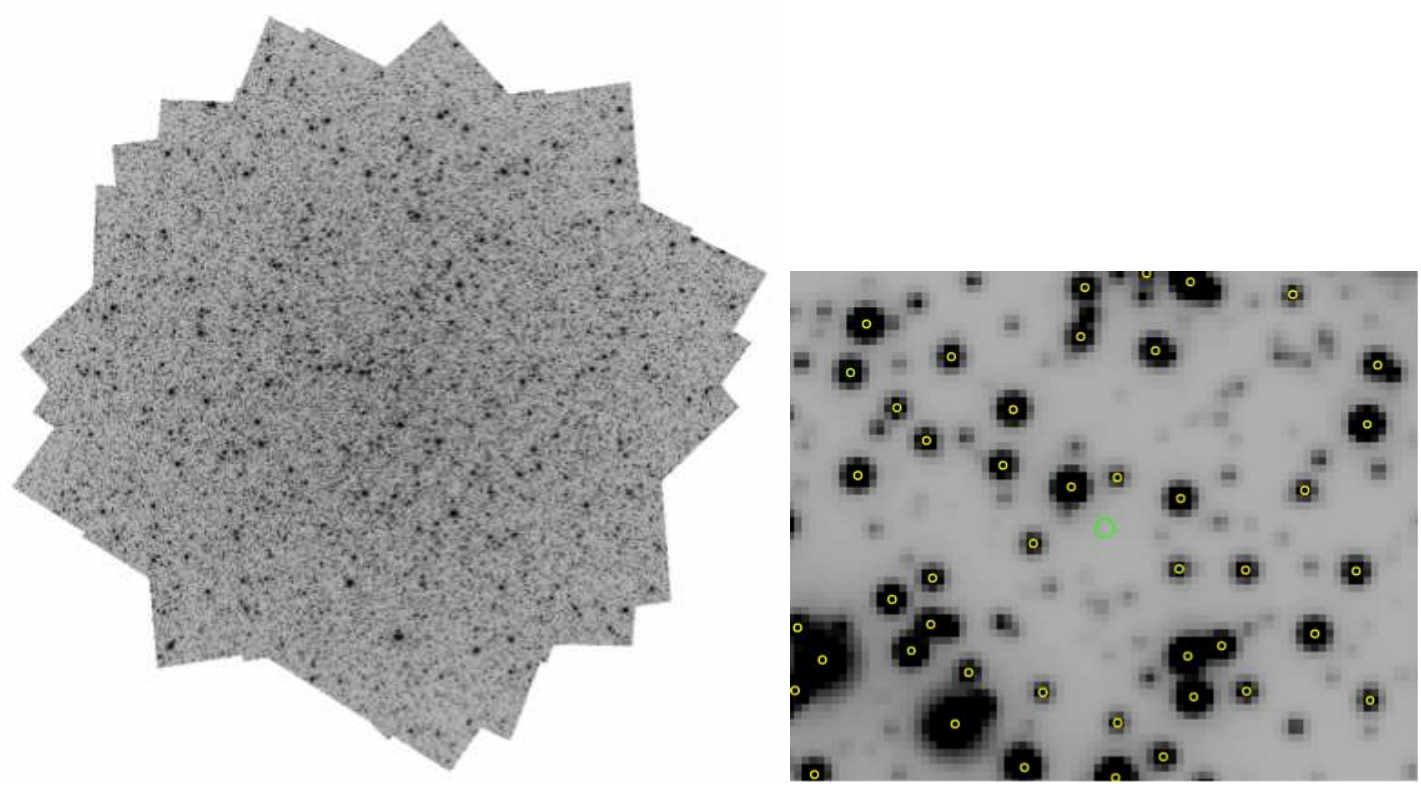

Fig. 3.— Left Panel: Stack image of all UVIS images used to create the master stars list. Right panel: Close up region around center of the cluster. Green circle indicates the center of the cluster and yellow circles indicate X&Y positions of well-measured stars.

3.3. Self-Calibration

The final master list of X&Y positions was used to cross-identify the X&Y positions of stars in the list from each UVIS individual exposure. As such, we arrived at an array of observations *XRAW[n,m]* and *YRAW[n,m]* and *MRAW[n,m]*, which are the raw flc-based

measurements of position and instrumental magnitudes and where n is the star number (which goes from 1 to 184,890) and m is the image number (which goes from 1 to 81). The challenge now is to take this multitude of observations and distill them into a single catalog of stars with average positions and errors.

The construction of a self-calibrated master frame is necessarily an iterative process. The mapping of X&Y positions from each frame into the X&Y positions from master frame depends on the positions of stars in the reference frame, but in order to measure positions for stars in the reference frame, we need to have accurate transformations of X&Y from each exposure into X&Y positions of that frame.

We start with the positions from the initial comparison. A 6-parameter linear transformation between each exposure and the reference frame using the bright, unsaturated stars in common:

$$U = X_0 + A{\times}X + B{\times}Y \tag{3}$$

$$V = Y_0 + C{\times}X + D{\times}Y \tag{4}$$

where U, V are positions from the reference frame and X,Y positions corrected for distortion from each UVIS exposure; X_0, Y_0 are offsets between the two systems; *A, B, C, D* are linear terms.

The determination of the transformation is also an iterative process, since every star is not measured well in every exposure. In determining the transformation, we iteratively reject the 5-sigma outliers until all residuals are within 5-sigma. We then take these 6-parameter transformations and turn them into 4-parameter conformal transformations by computing a new average linear terms as $A' = D' = (A - D)/2$, and $B' = -C' = (B + C)/2$. In addition to transformation of the positions, we also determine the magnitude zero-point for each exposure and adjust the fluxes accordingly. We then use these new transformations to estimate XBAR & YBAR, the master-frame position for each star found in each exposure. We compute a robust average of these position and flux estimates and set the new master-frame position to be: $X[N+1] = 0.25 * X[N] + 0.75 * XBAR$ and similar for Y[N+1], where N is number of iteration. We use a damping factor of 0.75 in an effort to prevent ringing in the convergence on the final master catalog.

With these new reference-frame positions, we re-compute the transformations for the next iteration. We performed 9 such iterations. After the first iteration, the typical residual was about 0.05 pixel. After the second, it was 0.03. After the fourth iteration it was 0.01, and after the ninth iteration it was less than 0.001 pixel.

The result of this exercise is that we now have a list of star positions and associated errors. Figure 4 shows the instrumental UVIS magnitude against the formal centering errors of X&Y-position. The stars brighter than $\lesssim$–14 instrumental magnitude are saturated, so that measured positions get extremely bad. For stars $-14 \lesssim$ mag $\lesssim -10$ have centroid

errors of X&Y-position less than 0.05 pixel in each coordinate. The centering error of X&Y positions is increasing with the fainter magnitude.

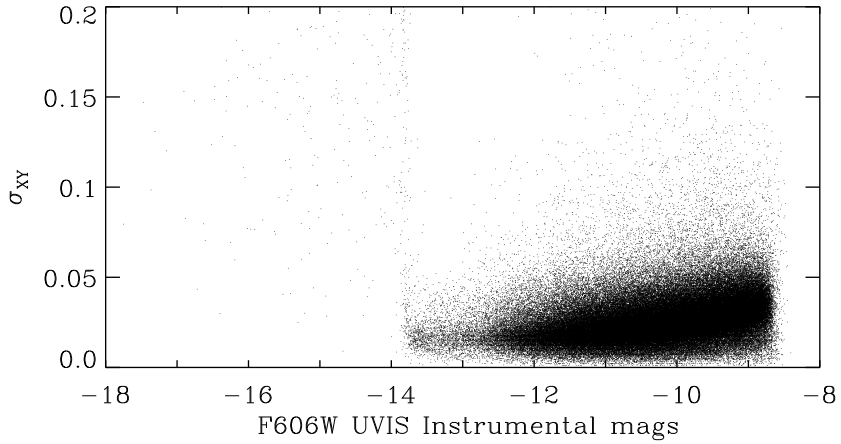

Fig. 4.— Formal centering errors of X & Y positions as a function of instrumental magnitude, for stars from the newly created master catalog. The stars brighter than about -14 magnitude are saturated. Stars $\gtrsim -14$ instrumental magnitude are well measured and the positions errors are less than 0.05 pixel in each coordinate. Position errors (σ_{XY}) are calculated as $\sqrt{(\sigma_X^2 + \sigma_Y^2)}$.

3.4. Proper Motion

Since the stars in ω *Cen* are moving with a dispersion of 0.9 *mas* or $\sim$0.02 pixel in each coordinate per year, it does not take long for the positions in this catalog to degrade over time. In an effort to keep this catalog usable for longer, we have used ACS observations taken in 2002 (GO-9442) and 2006 (GO-10775) to determine a proper motion for each star. To do this, we determined an average position for each star in each of the two early epochs. We computed a proper motion for each star for each epoch by comparing its early-epoch position against our master-frame position which can be associated with its average UVIS measured epoch. Figure 5 (upper left panel and upper right panel) shows the comparison of proper motions between the two independent epochs. The distribution along the 45 degree line indicates the proper motion itself, and the spread about this line indicates the errors. For the stars found in both data sets, we determined a motion by averaging the two estimates and determined an error by taking half the absolute difference between the two estimates. For the stars found in only one epoch and because of that have only one measurement, we adopted the measured motion and as its error we took the *RMS* at the measured epoch as

an upper limit on the quality of measurement. The bottom left panel in Figure 5 shows the measured proper motion for the stars with proper motion errors less than 0.01 pixel/yr. The plot on the bottom right in Figure 5 shows the distribution of the proper motion (number of stars) and their errors for stars found in both lists and only one or other. The data from 2006 set covered only the central area of the field, so many stars were found in 2002 but not in 2006.

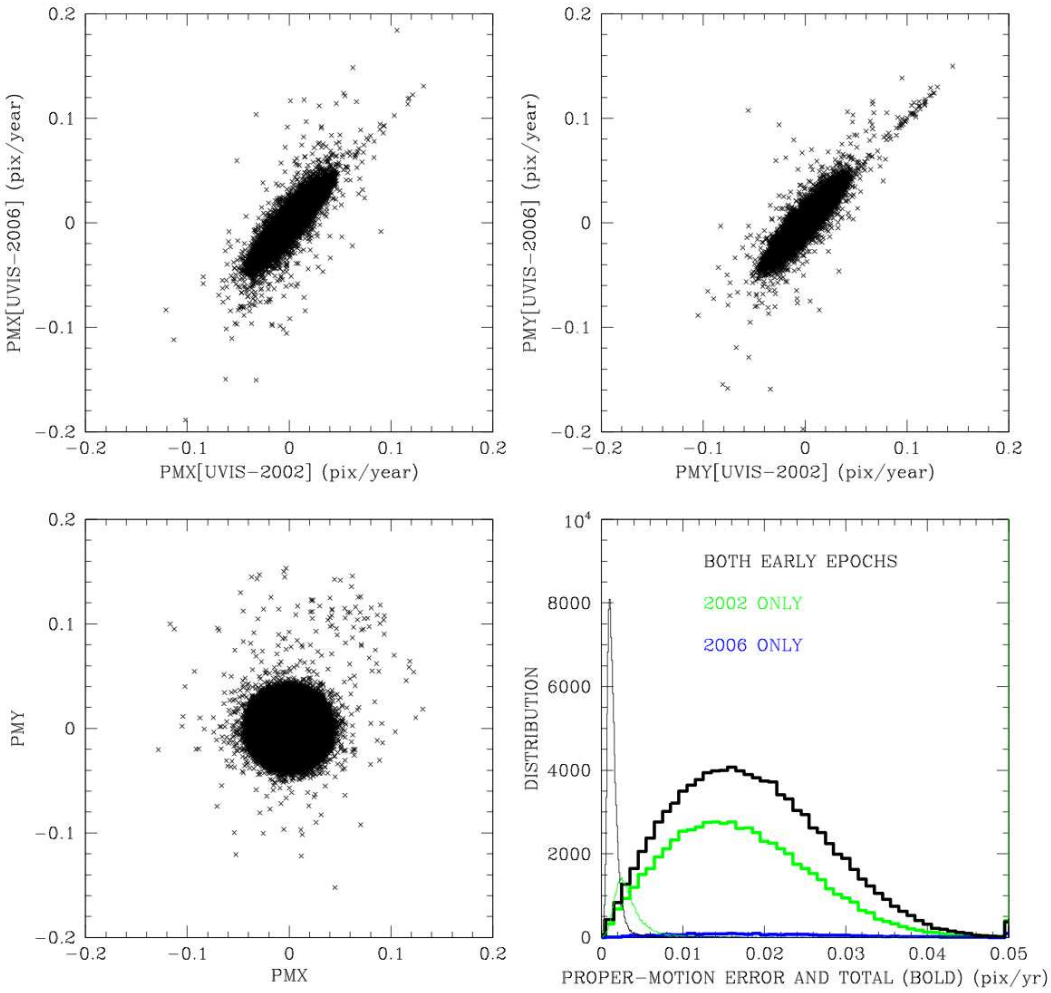

Fig. 5.— The upper left and right panels show the absolute difference in *PMX* and *PMY* between the two early epochs, respectively. The bottom left panel shows the measured proper motions for stars with proper–motion errors less than 0.01 pixel/yr. The bottom right panel shows the distribution of proper motions errors for stars found in all 3 epochs (black bold curve); the green curve shows only stars from 2002 epoch and the blue curve shows only stars from the 2006 epoch.

3.5. Description of the Catalog

The catalog derived above is available in the form of a simple text file, with the name FINAL_CATALOG.XYM_PM. It contains the average position and instrumental magnitude for each star, the *RMS* of the individual estimates that went into this average, and the number of exposures available for each star. It also provides the average "epoch" *TBAR* for UVIS observations, proper motion and the sigma of the proper motions, namely:

COL01: XMASTER (50 mas/pixel, along E)
COL02: YMASTER (50 mas/pixel, along N)
COL03: MMASTER (F606W ; 40s exposure)
COL04: RMS(XMASTER)
COL05: RMS(YMASTER)
COL06: RMS(MMASTER)
COL07: NOBS(number of the observations)
COL08: TBAR(the average epoch of observations)
COL09: PMX (x proper motion in pix/yr)
COL10: PMY (x proper motion in pix/yr)
COL11: ePMX (error in proper motion in pix/yr)
COL12: ePMY (error in proper motion in pix/yr)

4. Validation of the WFC3/UVIS Distortion from Drizzled Images

The official geometric–distortion correction for the WFC3/UVIS images is used in the STScI on-the-fly pipeline (OTFR) as the reference file IDCTAB (Instrument Distortion Coefficients Table) and based on Kozhurina-Platais *et al.* (2009) solution. The purpose of the WFC3 linear geometric distortion validation is to investigate whether there are any changes in the distortion and, if so, to determine how significant they are, and how accurate the UVIS images can be mapped with the new ST software *DrizzlePac/AstroDrizzle* (Gonzaga, *et al.* 2012). It is important to look for any systematic residuals, such as the X,Y scale change over time, from the single drizzled UVIS image.

4.1. Reductions

Firstly, all images were processed through the pixel-based CTE correction, (Anderson & Bedin, 2011), described in Sec. 3.1. Secondly, the header for all `*_flc.fits` images were updated using the new and improved WFC3/UVIS geometric distortion (Kozhurina-Platais, 2014) which includes:

- the pixel–grid irregularities due to the lithographic pattern, presented in the form of a 2-D look-up table (reference file D2IMFILE);
- the improved geometric distortion polynomial coefficients in the form of a reference file IDCTAB (Instrument Distortion Correction Table);
- the non-polynomial, filter-dependent part of the distortion presented in the form of a 2-D look-up table (reference file NPOLFILE).

The *DrizzlePac/AstroDrizzle* software uses all UVIS geometric distortion reference files and outputs that result into the individual ∗_single_sci.fits UVIS images, which are now corrected for distortion.

The X&Y positions from each UVIS individual drizzled image (∗_single_sci.fits) were obtained using the IRAF/DAOPHOT/PHOT task with CENTERPARS which includes a 2D-Gaussian fit to the PSF and simultaneously performs aperture photometry. The output from this taks is the list of X&Y positions, the centering errors of the 2-D Gaussian fit and measured instrumental magnitude $Inst.mags = -2.5log(\frac{Flux}{Exp.Time})$ for each stars. Figure 6 shows that the formal measuring precision of the X&Y position as a function of instrumental magnitude provides a reasonable positions errors even for the undersampled UVIS PSF.

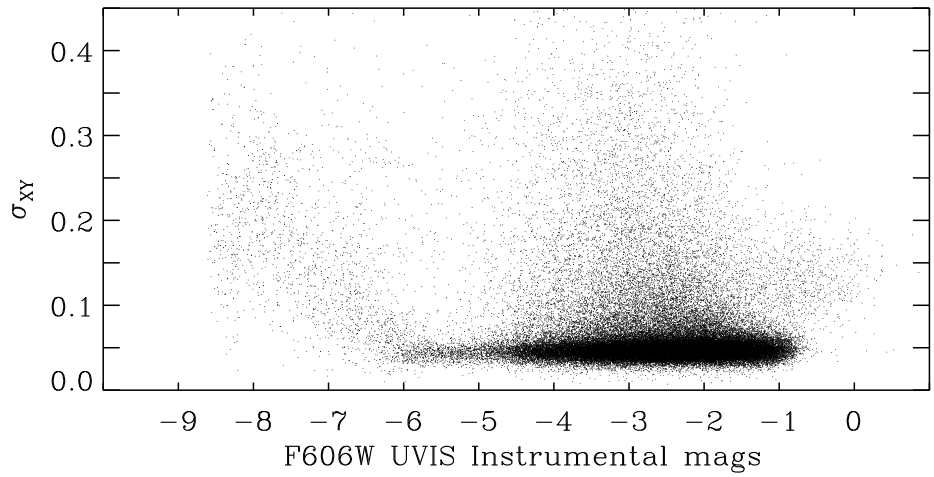

Fig. 6.— Formal centroid X&Y errors as a function of instrumental magnitude, for stars from a single UVIS drizzled image. The points above the general trend of astrometric error ($\sigma_{XY} \gtrsim 0.1$ and for $-5.0 \lesssim$ mag $\lesssim -1$) are likely to be cosmic rays. The stars brighter than about −6 magnitude are saturated. Positional errors (σ_{XY}) are calculated as $\sqrt{(\sigma_X^2 + \sigma_Y^2)}$.

A total of 60,000 stars were measured in each of the single–UVIS–drizzled image. This is a sufficient number of stars to look with confidence for systematic errors in the UVIS X&Y positions.

4.2. Geometric Distortion of the WFC3/UVIS: Analysis of the Linear Part

Most of the distortion in WFC3/UVIS is non-linear, but there are two linear terms that must be validated. These two linear terms correspond to the the difference in scale between the principal X&Y axes and the non-orthogonality between the X&Y axes .

In order to validate the WFC3 geometric distortion and test for possible residual systematic errors, we used the linear transformation (Eq.3–4 in Sec. 3.3), where U & V are the positions from the standard astrometric catalog on a rectangular coordinate system free of any systematics, and X & Y are the measured positions from single–UVIS–drizzled image, corrected for distortion. Then, the rotation angle between these two systems (Taff, 1980) can be defined as:

$$\tan(\theta) = \frac{B}{C} \tag{5}$$

The plate-scale term by default is defined as:

$$\mathcal{M} = \sqrt{(A \times D - B \times C)} \tag{6}$$

As described in Anderson (2007), the on–axis skew, which represents the difference in the scale between the X,Y axis is defined:

$$\mathcal{M}_{on-axis} = \frac{A - D}{2} \tag{7}$$

The off–axis skew, representing non-perpendicularity between the X,Y axis is defined:

$$\mathcal{M}_{off-axis} = \frac{B + C}{2} \tag{8}$$

Thus, the skew terms defined above are the parameters used to characterize the linear part of geometric distortion and the accuracy of geometric distortion reference files for the WFC3/UVIS, adopted in the STScI on-the-fly pipeline (OTFR). If the linear terms are properly calibrated in the UVIS distortion model and constant over time, then these two skew terms measured by comparing each single-UVIS-drizzled exposure to the reference frame should show just a random scatter around zero and should not have trend over time.

4.3. Testing the Skew Terms in UVIS Drizzled Images

A simple way to estimate the skew terms, discussed in Sec.4.2, is to compare the derived positions for stars in the observed UVIS frames with their counterparts in the reference frame.

Thus, all observations of ω *Cen* taken over five years were drizzled into a single–UVIS –drizzled image, as described in Sec.4.1. Then the measured positions derived from a single–UVIS–drizzled image, were mapped into the positions from standard astrometric catalog, solving for 3×2 parameters in Eq.3–4. During each solution cosmic rays, saturated stars, hot pixels and spurious detections (Fig.6), were iteratively rejected from the data as extreme outliers with residuals exceeding ~ 0.1 pixels. Each solution with well-measured stars yielded the *RMS* of linear fit at the level of ~ 0.03 ACS/WFC pixel (or 1.5 *mas*), shown in Figure 7.

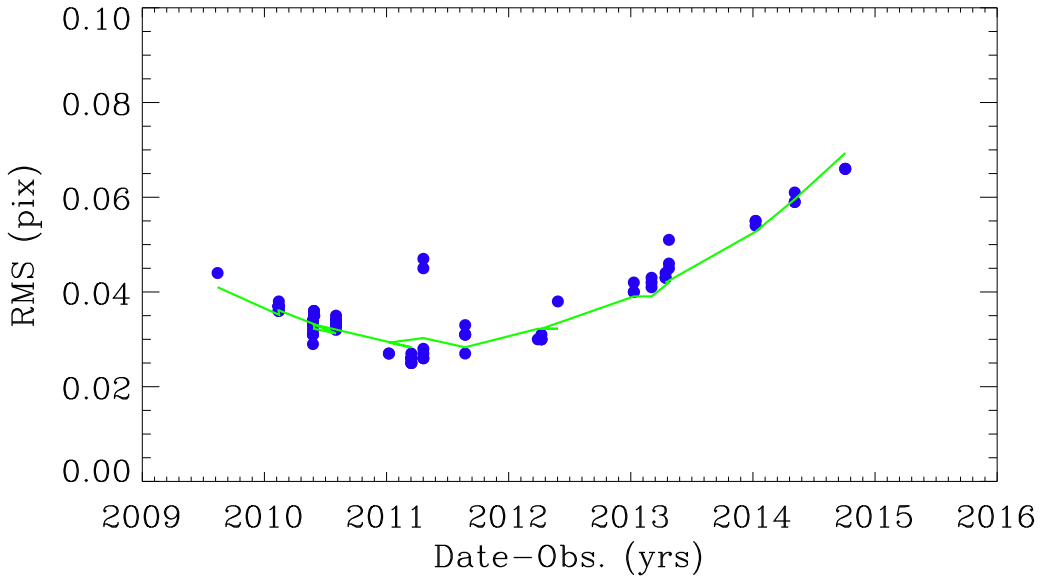

Fig. 7.— *RMS* from the linear solution as a function of time for each UVIS-drizzled-images of ω *Cen* taken through F606W filter. The units of Y-axis are ACS/WFC pixels.

As can be seen in Fig.7, the *RMS* of solutions appears to be gradually changing with time from the minimum ∼0.025 ACS/WFC pixel (in $\sim$ 2011.5) to the maximum of ∼0.066 ACS/WFC pixel (in $\sim$ 2015). The trend in the *RMS* of solution is the indication of the internal motions of stars in ω *Cen*. As reported by Anderson & van der Marel (2010), the

internal velocity dispersion in the proper motions of ω *Cen* is at the level of 0.9 *mas* per year. The average epoch of the standard astrometric catalog is ∼2011, as described in Sec.3. Thus, the epoch difference between each WFC3/UVIS observation of ω *Cen* and the standard catalog range between 2 to 4 years. The resulting displacement scales up proportionally with the epoch difference and hence, the epoch difference of 2 years on average contributes to the *RMS* as much as ∼2 *mas* or 0.045 ACS/WFC pixel.

In order to look for any changes in the linear part of distortion, we calculated the skew terms from Eq.7–8, (scaled by 2048 to provide the effect of displacement at the far edge of UVIS drizzled image). These terms are plotted as function of time in Figure 8.

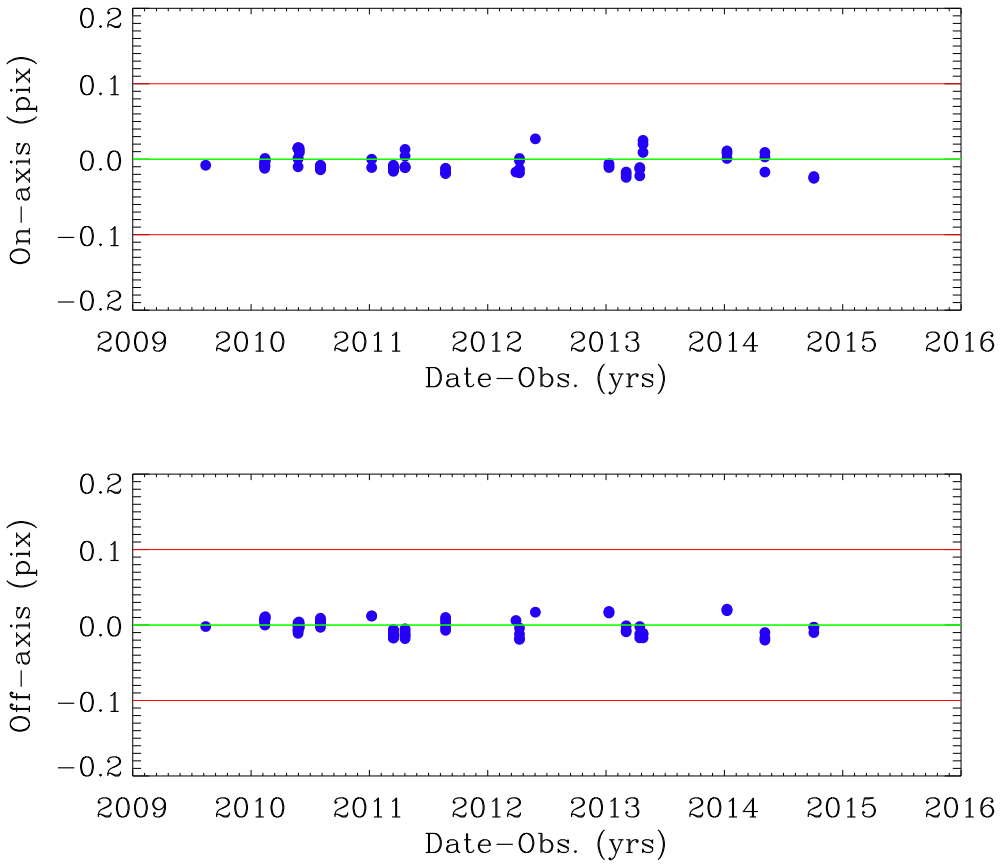

Fig. 8.— Calculated skew terms from Eq.4–5 as a function of time, top on–axis skew and bottom off–axis skew, respectively. Each point represents the calculated skew terms from the solution and is scaled to 2048. The over-plotted red lines at the level of ±0.1 pixel indicate the specification of *Astrodrizzle* (∼ 0.1 pixel) on the accuracy for alignment of HST images. The units of Y-axis are ACS/WFC pixels.

These two scale-related terms (on–axis and off–scale skews), appear to be consistent with zero amount of skew and are constant over 5 years of UVIS observations. However, the skew calculated from observations within three consecutive HST orbits (CAL-12094, 24th April 2010, total period of time ∼3 hours) exhibits a linear trend of the skew, linearly correlated with the location within an HST orbit. As discussed in Sec 4.3 of Kozhurina-Platais & Petro (2011, see Fig.4–5), there are clear indications of linear dependency with the HST orbital time due to the telescope breathing, which takes place on orbital time-scales and causes small but detectable changes of focus and PSF shape. Due to orbital breathing, the UVIS scale varies from image to image with linear and periodic deviations reaching ±0.05 pixel (±2 *mas*) at the far edge of UVIS drizzled images. Velocity aberration is another factor that contributes to the scale change in the UVIS images (Cox & Gilalland, 2002). However, the velocity aberration is a known correction factor to the image, and it is available in the header of the science *fits* file and is used by *DrizzlePac/AstroDrizzle*. Thus, the linear terms calculated from the UVIS drizzled images should be velocity aberration free.

One of the errors in the linear part of distortion is related to the plate-scale. In Figure 9, the plate–scale is shown as a ratio of the plate–scale between the standard catalog (0.″05/pix) and each individual drizzled UVIS image (0.″04/pix). The calculated plate–scale (Eq. 6) as seen in Fig. 9, appears to be slightly changing over time, which is probably related to a focus drift. The deviation in the plate-scale over time is so insignificant that it can be adopted as a constant.

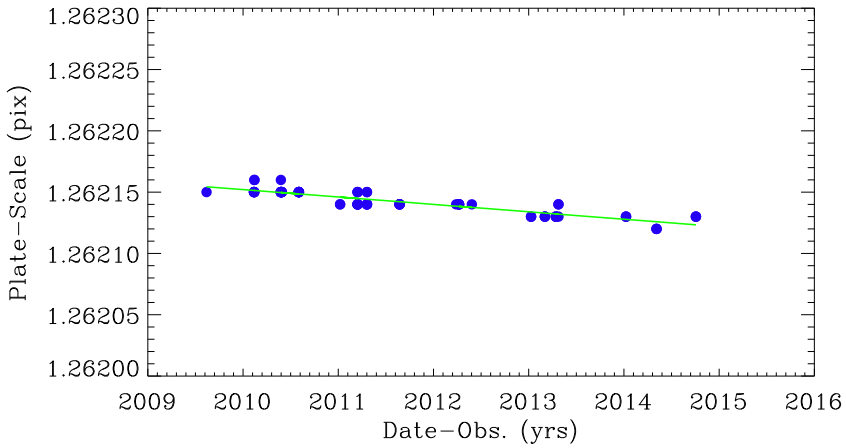

Fig. 9.— Calculated plate–scale from Eq. 6, as a function of time. Each point represents the calculated plate–scale from the linear solution for a given single-UVIS-Drizzled image. The over-plotted green line corresponds to the linear fit of the plate–scale between standard astrometric catalog and each individual–UVIS–drizzled image.

Another systematic error in the geometric distortion model is the error related to the rotation angle (Eq. 5) between the standard catalog and drizzled images. The orientation angle of HST images is one of the critical parts of the astrometric calibration. HST is a free-flying telescope and the focal plane axis of the telescope is defined in terms of the *V2* & *V3* plane. If the HST roll-angle is 0, the *V3* axis is parallel to North. Thus, the angle in the geometric solution defined in the linear part of the distortion must to be accurately calibrated, and if there are errors in the linear part of the solution, it will introduce errors in the angle between the standard astrometric catalog and any UVIS drizzle images. Figure 10 shows the difference between the orientation angle measured in the standard catalog and that from PA_V3 in the image header for each image.

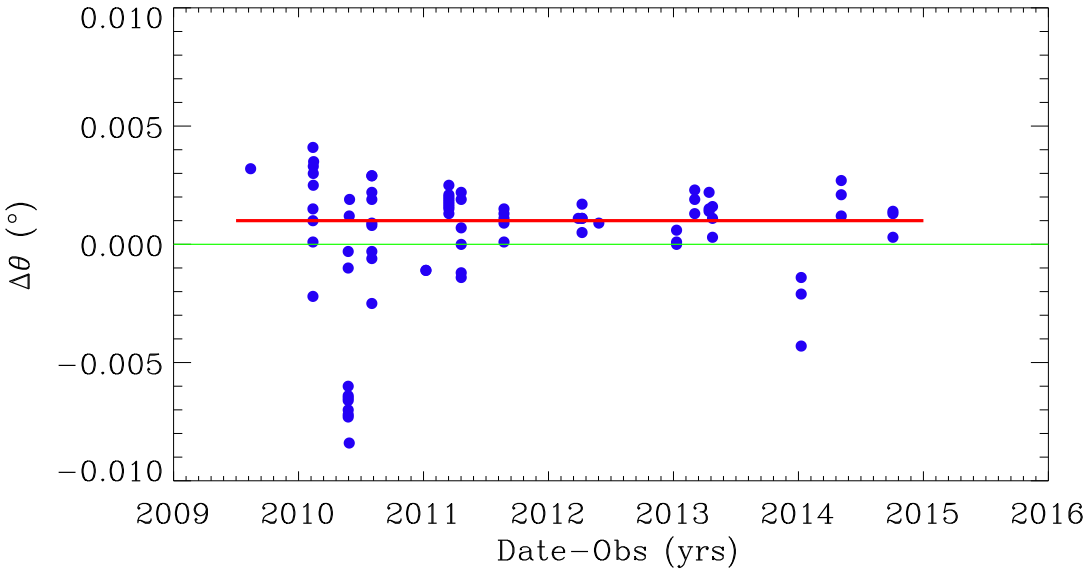

Fig. 10.— Rotation angle between the standard astrometric catalog and each individual–UVIS–drizzled image as function of time. Each point represents the calculated rotation angle from each solution. The over-plotted red line corresponds to the median offset in the rotation angle.

As seen in Figure 10, the angle between the standard catalog and each single–UVIS–drizzled image is around $0\overset{\circ}{.}001$ (or $3\overset{''}{.}6$). The offset by this amount could be explained by either the standard catalog being off or the WFC3/UVIS IDCTAB being off. It is more likely that the standard astrometric catalog is off, since its absolute orientation was fixed into the system of Two Micron All Sky Survey (2MASS (Skrutskie et al., 2006)), which currently is the best representative of the International Celestial Reference System (ICRS) on very short spatial scale (like the FOV of HST). On the other hand, the absolute astrometric coordinate

system of HST is known to be good to only about 1-2″ due to the errors in the HST guide-star catalog. There is also a noticeable deviation at $-0\overset{\circ}{.}008$. This large deviation of the angle took place on 28th April 2010 (CAL-11911), when ω *Cen* cluster was observed with large pointing offsets (*POS TARG*) $\pm 40''$. The guide-star acquisition failed during the large dithered observations and, as a result, the telescope lost pointing accuracy and it caused the HST roll-angle deviations of $0\overset{\circ}{.}008$ from the nominal of $\sim 0\overset{\circ}{.}003$.

Summarizing the analysis of UVIS skew terms, we found that there is no indication that the skew terms in the WFC3/UVIS geometric distortion solution in the form of IDCTAB (Kozhurina-Platais, 2014) are either in error or variable over time (apart from the breathing phenomenon). The plate–scale is stable and well calibrated. Finally the orientation of the WFC3/UVIS detector to the focal plane axis of the telescope is also stable over time and consistent with the catalog to better than $0\overset{\circ}{.}001$.

5. Conclusions

Five years of ω *Cen* observations through F606W WFC3/UVIS filter have been used to create a standard astrometric catalog and examine the linear part of the WFC3/UVIS geometric distortion and the variation of the X&Y scale over time. The resulting X&Y scale terms, one of the major components in the geometric distortion, have been calculated from the comparison of all observations of the ω *Cen* over 5-years and the newly created standard astrometric catalog.

These comparisons show that UVIS skew terms are stable over a 5-year time period, further indicating that the UVIS geometric distortion solution is accurate and precise at the level of 1 *mas*. If any of the geometric distortion component presented in the form of the reference files (IDCTAB, D2IMFILE, NPOLFILes) used in *AstroDrizzle/DrizzlePac* were not accurate and contained any significant uncertainties, then that would have introduced systematic errors, e.g., offsets in the UVIS skew terms in the solution between the standard catalog and each UVIS–drizzled images.

Summarizing the assessment of the linear part of WFC3/UVIS geometric distortion, we conclude that over 5 years of the WFC3 operation on-board the HST, the WFC3/UVIS geometric distortion is time–independent and not exhibiting sudden changes or fluctuation. On the top of that, however, there are linear and periodic deviations at the level of ± 0.05 pixel (*2mas*), related to the orbital breathing.

However, even with a perfectly accurate distortion solution, the precision of astrometry with WFC3/UVIS images depends critically on the technique used to measure individual star positions in under-sampled WFC3/UVIS and WFC3/IR images. Errors related to the under-sampled UVIS PSF can easily be larger then those due to errors in distortion correction.

The stability of the WFC3/UVIS provides a stark contrast to the well–established mono-

tonic variation of the ACS/WFC skew terms (Anderson, 2007)that has been observed since ACS was installed in 2002. The size of the ACS/WFC skew terms change was clearly noticeable over 5 years at about 15 *mas* off from the original 2002-based distortion solution, whereas the WFC3/UVIS skew over 5 years of observations is consistent within zero, accurate and stable at the level of $\pm 2 mas$. The WFC3 instrument is designed for a high degree of mechanical and optical stability. The optical bench structure is extremely stiff and not subject to the dimensional effects due to water desorption in prior HST instruments. More importantly, the entire structure is encased within a thermal enclosure. This provides both a colder environment to reduce thermal infrared radiation (significant at the longest wavelengths of the IR channel) and also excellent thermal stability ($\ll$ 1C). This combination, together with the favorable location within the HST spacecraft, results in a very stable optical system.

Acknowledgments

We thank John MacKenty for his keen interests in the construction of standard astrometric catalog based on UVIS observations and for his encouragement in the examination of the WFC3/UVIS geometric stability. V.K.-Platais especially appreciates the lengthy discussions with John MacKenty related to the instrumental and technical issues of the WFC3/UVIS camera. V.K.-P. is thankful to W. Januszewski for the help in designing of several calibration programs which required an incremental step of HST roll–angle. V.K.-P. is thankful to Andrea Bellini for careful reading of the early version of this report for useful suggestions, which significantly improve and clarify the text. We gratefully acknowledge Mike Fall and Elena Sabbi for reviewing this ISR and for their very valuable comments.

References

Anderson, J., 2006, ACS Instrument Science Report, ACS-ISR-06-01 (Baltimore:STScI)

Anderson, J., 2007, ACS Instrument Science Report, ACS-ISR-07-08 (Baltimore:STScI)

Anderson, J., & van der Marel, R.P., 2010, ApJ, 710, 1032-1062

Andesron, J., & Bedin, L., 2010, PASP, 122,1035

Bellini, A., Andesron, J., Bedin, L.R., 2011, PASP, 123, pp.622-637

Cox, C., Gilliland, R., 2002, in 2002 HST Calibration Workshop, eds. A.Arribas, A. Koekemoer, B.C. Whitmore (Baltimore:STScI), p.58

Gonzaga, S., et al., 2012, "The DrizzlePac Handbook", (Baltimore:STScI)

Harris, W.E. 1996, AJ, 112, 1487

Kozhurina-Platais, V., Goudfrooij, P., Puzia, T., 2007, ACS-ISR-07-04 (Baltimore:STScI)

Kozhurina-Platais, V., Cox, C., McLean, B., Petro, L., Dressel, L., Bushouse, H., Sabbi, E., 2009, WFC3 Instrument Science Report, WFC3-ISR - 09–33 (Baltimore:STScI)

Kozhurina-Platais, V., Cox, C., Petro, L., Dulude, M., Mack, J., 2010, in 2010 HST Calibration Workshop, eds S. Deustua, C. Oliveira (Baltimore:STScI)

Kozhurina-Platais, V., Petro, 2012, WFC3 Instrument Science Report, WFC3-ISR - 12–03 (Baltimore:STScI)

Kozhurina-Platais, V., 2014, WFC3 Instrument Science Report, WFC3-ISR - 14–12 (Baltimore:STScI)in

Skrutskie, M.F., *et al.*, 2006, AJ, 131, 1163

Taff, G., L., 1980, in Computational Spherical Astronomy, John Wiley Sons, Inc, USA.